


**Bouncing of Leidenfrost steel balls on water surface**Chin-Chi Hsu (許進吉) <sup>\*</sup>, Shih-Hsien Cheng (鄭世賢), Yu-Feng Ko (葛昱鋒), Z-Hao Tsou (鄒子顥), Zhao-Chen Zhang (張兆辰), Chung-Jen Su (蘇崇仁), and Hong-Wei Chen (陳泓瑋)*Department of Mechanical Engineering, National United University, No. 2, Lienda, Miaoli 36063, Taiwan*

(Received 7 November 2023; accepted 13 June 2024; published 18 July 2024)

A steel ball with a density higher than that of water can bounce on a water surface when heated to a temperature well above the Leidenfrost point. In this letter, an experiment is conducted where heated steel balls are released onto a water surface. The heated steel ball descends into the liquid, thus causing the liquid to evaporate and form a vapor cushion with an upward force that lifts the steel ball. Subsequently, the steel ball bounces off the water surface, like a solid ball bouncing off an elastic surface without sinking into the water. This phenomenon is known as the inverse Leidenfrost effect. In this letter, we evaluate the various motion behaviors of spheres at different Reynolds numbers and temperatures. Additionally, we analyze the bouncing behavior of solid spheres on a free liquid surface and examine the various force components.

DOI: [10.1103/PhysRevE.110.L012802](https://doi.org/10.1103/PhysRevE.110.L012802)

When a droplet is deposited on an extremely hot solid surface, a vapor layer is created between the droplet and solid surface, thus allowing the droplet to levitate on the surface. This phenomenon, which was discovered in the 18th century, is known as the Leidenfrost effect [1]. Authors of numerous studies have demonstrated that the Leidenfrost effect can effectively reduce the heat transfer between liquid droplets and substrates, thus rendering it applicable in various engineering fields such as sublimation heat engines [2] and fire-suppression systems [3]. However, it adversely affects certain processes, such as nuclear reactions [4] and spray cooling [5]. Furthermore, the unique dynamic behaviors caused by the Leidenfrost effect, such as almost frictionless motions [6], self-propulsion [7], and drag reduction [8], have demonstrated substantial potential in transportation, including self-propelled vehicles [9], hovercraft [10], and energy conversion [11]. Therefore, further research and applications related to the Leidenfrost phenomenon can advance engineering and scientific technologies. Researchers have extensively investigated the bouncing dynamics of liquid droplets on solid surfaces [12–15]. Droplets and vapor coexist in the quasistatic Leidenfrost equilibrium; this phenomenon is governed by the relationship among the droplet shape, vapor-cushion thickness, gravity, surface tension, and the lift generated by vapor expulsion [14]. Bouillant *et al.* [13] reported that volatile liquids deposited on a thermally graded substrate were not only suspended (Leidenfrost effect) but also accelerated spontaneously toward colder regions.

In another scenario, when a hot object descends into a liquid with a low temperature or at boiling point, the evaporation of the working fluid creates a vapor film surrounding the hot object, thus reducing the dynamic drag of the fluid. This phenomenon is known as the inverse Leidenfrost effect [16,17]. The inverse Leidenfrost effect involves a hot object,

such as a droplet, levitated above a cooler liquid. In this case, the heat from the droplet causes some of the liquid to evaporate, thus forming a vapor cushion. Vakarelski *et al.* [18–21] investigated this topic comprehensively. They observed that heating steel balls descending into various liquids resulted in the formation of a vapor film enveloping the spheres and altered the shape of their wakes. Flow separation occurred near the upper pole, thus changing the pressure distribution around the spheres and reducing drag. The maximum drag reduction effect was 85%, with a 75% drag reduction in water near saturation temperatures. This effect was particularly pronounced at higher Reynolds numbers (Re) [18]. Additionally, they discovered that altering the wettability of a steel ball surface to render it either hydrophilic or hydrophobic substantially affected the persistence of the vapor layer. The vapor layer collapsed shortly after its descent for both hydrophilic and typical hydrophobic spheres [21]. However, the superhydrophobic spheres maintained the vapor layer throughout the descent until the temperature decreased to the pool temperature without transitioning to nucleate boiling during the process.

In a previous study pertaining to inverse Leidenfrost phenomenon in liquid-liquid systems [22], researchers reported that the pressure drop in the lubricating vapor layer can be expressed as  $\Delta P \sim \frac{\mu \Delta T R^2}{h^4}$ , where  $\Delta P$  is the pressure within the vapor layer,  $\mu$  the viscosity,  $\Delta T$  the temperature difference,  $R$  the sphere radius, and  $h$  the vapor film thickness. This pressure drop governs the suspension and sinking behavior of the droplets. The levitation time exhibits a linear relationship with the droplet radius. Furthermore, in the experiments conducted by Gauthier *et al.* [23], ethanol droplets self-propelled when deposited on liquid nitrogen, which was attributable to the instability of the droplet at the liquid-nitrogen interface (caused by the thickness of the thin film  $\Delta h$  before and after the droplet was deposited). This contrasts with the motion observed on solid substrates, which is driven by the symmetry breaking of internal flow within the droplet [24].

<sup>\*</sup>Contact author: [cchsu@nuu.edu.tw](mailto:cchsu@nuu.edu.tw)

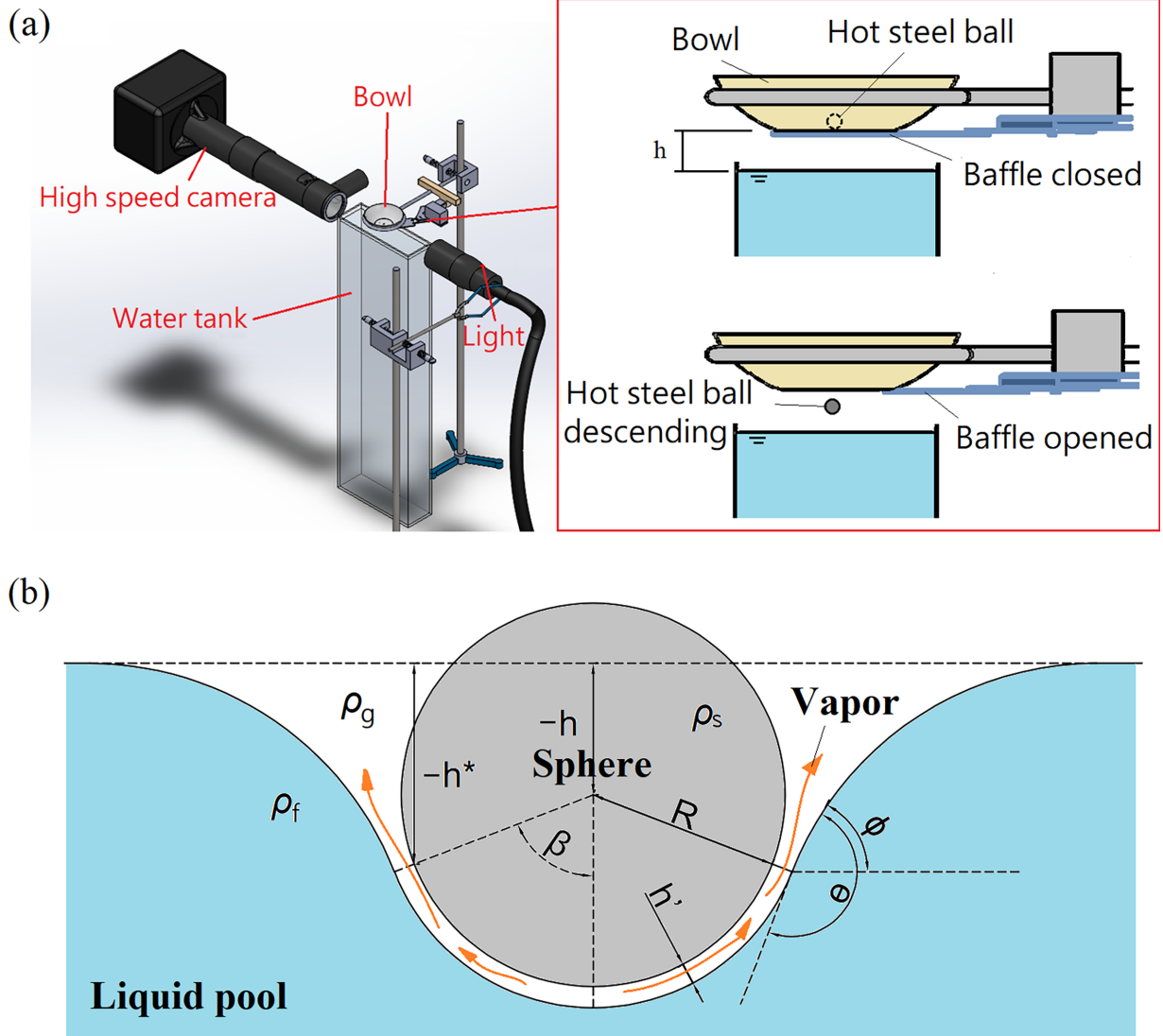


FIG. 1. (a) Setup for descending-sphere experiment; subfigure shows control of descending heated sphere. (b) Sphere with temperature higher than Leidenfrost point can generate a vapor film, thus resulting in the inverse Leidenfrost effect.

Lee and Kim [25] investigated the impact of solid spheres on a free liquid surface and discovered that solid spheres with a higher density can bounce on the free surface of a liquid with a relatively lower density without sinking into the water. This is attributed primarily to the superhydrophobic surface of the steel ball used. This letter is based on this observation. Specifically, the purpose of this letter is to investigate whether steel balls heated to the Leidenfrost temperature can bounce on the surface of water. In previous experiments involving spheres descend freely into water, researchers typically focused on the cavity depth and meniscus [26–29]. In this letter, we investigate the dynamic behavior of solid Leidenfrost metal spheres on a liquid surface. Specifically, millimeter-sized spheres are heated to reach the Leidenfrost temperature, fixed to a specific height, and allowed to descend freely. We discovered that, once high-density metal spheres reached a specific Leidenfrost temperature, they bounced on the water surface without sinking. Thus, we endeavor to determine the factors contributing this bouncing behavior of high-density metal spheres.

Figure 1(a) shows a schematic illustration of the experimental setup for this letter, which is inspired by the setups used by Aristoff and Bush [28] and Castagna *et al.* [30]. The tank was filled with water, and a high-speed camera was strategically positioned to capture the front view of the tank. Various small steel balls with diameters ( $D$ ) of 0.5, 0.7, 1, and 2 mm were heated and released freely from heights ( $H$ ) of 1 and 0.5 cm above the water surface. In this setup, we devised a simple mechanism to control the ball descent. A heat-resistant bowl with a diameter of 2.2 mm at the bottom was placed directly above the tank. A baffle was used to conceal the hole, and small steel balls were placed in the bowl through the hole using pliers. A heat gun was utilized to heat the steel ball positioned above the bowl. The temperature was measured using an infrared thermometer. When the ball reached the desired temperature (450, 550, 560, 580, and 600 °C), the heat gun was turned off, and the baffle was swiftly adjusted to open the hole, as shown in the subfigure of Fig. 1(a). This allowed the heated ball to descend smoothly into the tank. The entire process was recorded using a high-speed camera at 2000 fps.

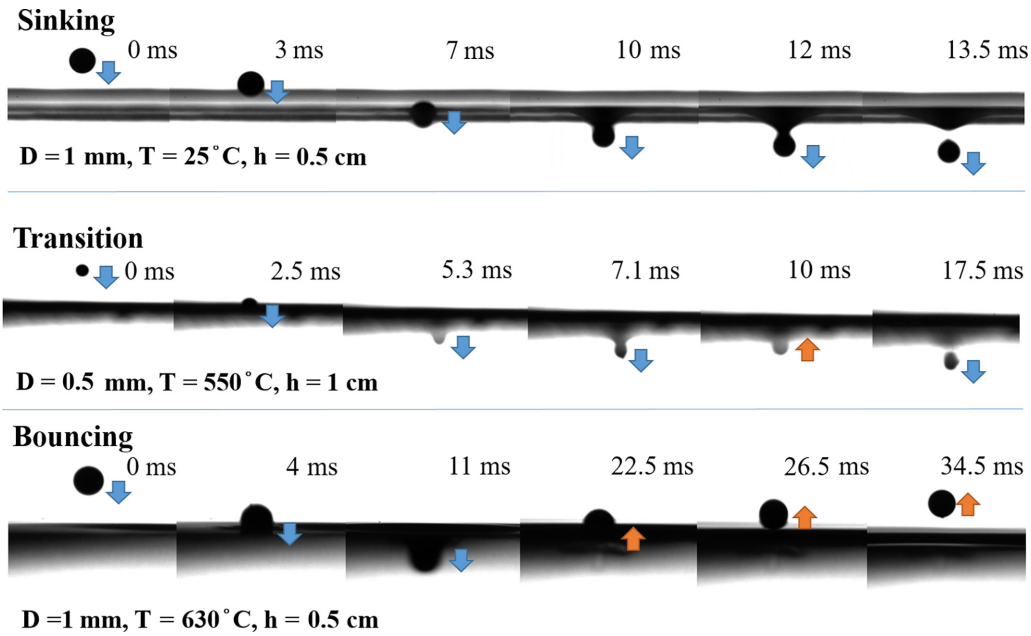


FIG. 2. Three sets of images showing a ball of different sizes descending into water at different heating temperatures and release heights. The phenomenon of a heated ball impacting water surface can be categorized into three scenarios: sinking, transition, and bouncing. The video in the Supplemental Material [33] shows the moving images of this figure.

When the temperature of the sphere was  $25^{\circ}\text{C}$  and the sphere was extremely small, the impact velocity was extremely low, and surface tension dominated the dynamic behavior of the sphere after it impacted the surface. In this case, the sphere may either float or bounce [25]. Authors of other studies showed a similar behavior for liquid droplets impacting a free liquid surface, thus indicating the presence of an air layer enabling the floating or bouncing behavior [31]. In the experiments, we observed that, as the temperature increased, oscillations occurred near the saturation temperature and disappeared completely at  $150^{\circ}\text{C}$ . These oscillations were primarily caused by surface tension. Oscillations describe the phenomenon where a sufficiently small sphere, when released onto the surface of water at room temperature, becomes trapped on the liquid surface owing to surface tension, thus preventing it from sinking or bouncing [31]. When the temperature of the sphere is lower than the boiling temperature of water, the main factor determining the ability of the sphere to oscillate is surface tension. As the inertia and gravity acting on the sphere during the descent increase, the surface tension of the water becomes insufficient to support the sphere against these forces, thus resulting in the sinking of the sphere.

However, when the temperature of the sphere is significantly higher than the Leidenfrost temperature, as shown in Fig. 1(b), the sphere begins to levitate on a layer of vapor, which is generated from the evaporation of the pool surface. The heat released by the sphere is transferred to the pool surface; subsequently, the vapor generated from evaporation flows outward through the gap between the sphere and liquid pool. The pressure field generated within the vapor layer (driving the flow) governs the levitation of the sphere. Here,  $\beta$  represents the half of overlapping contact angle [32],  $\theta$  the contact angle between the sphere and liquid in the pool,  $\phi$  the interfacial inclination angle,  $h^*$  the height from the liquid level to the contact point,  $h'$  the vapor film thickness,  $h$  the

instantaneous depth,  $\rho_f$  the density of water,  $R$  the sphere radius,  $\rho_g$  the vapor density, and  $\rho_s$  the steel-ball density.

In this letter, we observed three phenomena, i.e., sinking, transition, and bouncing, when hot spheres experienced the Leidenfrost effect and descended into the water surface, as depicted in Fig. 2. Sinking was observed when the hot steel ball ( $D = 1\text{ mm}$ ,  $T = 550^{\circ}\text{C}$ , and  $H = 0.5\text{ cm}$ ) descended into the free liquid surface, and its motion direction and velocity continued downward until the vapor cavity formed by the crescent shape was pinched off, thus causing the sphere to sink completely into the water. The surface temperature of a heated steel ball significantly affects the bouncing phenomenon. Hence, when the temperature of the steel ball ( $D = 1\text{ mm}$  and  $H = 0.5\text{ cm}$ ) reached  $\sim 600^{\circ}\text{C}$ , the upward vapor pressure force generated by the film was sufficient to allow the steel ball to overcome gravity and inertia, thus allowing it to bounce on the surface of the water. The upward force was caused by the vapor pressure force generated by the vapor film [22]. The main difference between bouncing and sinking is that, after the steel ball reaches the free liquid surface, its downward velocity decreases to zero when it reaches a specific position on the crescent surface. An upward velocity is generated until the sphere departs from the free surface.

However, as the diameter of the small steel ball decreased ( $D = 0.5\text{ mm}$  and  $T = 550^{\circ}\text{C}$ ), a transition may occur. When the steel ball reached its maximum cavity depth, it traversed upward and then oscillated on the free liquid surface. We believe that the vapor layer remained present at this time. Over time, the decrease in vapor generation reduces the lift necessary to suspend or bounce the sphere on the liquid surface, thus ultimately resulting in the sinking of the sphere. To establish a relationship between the vapor pressure caused by temperature and the inherent inertial force of the sphere during its descent, we conducted a dimensional analysis and discovered that the inertial force of the steel ball was

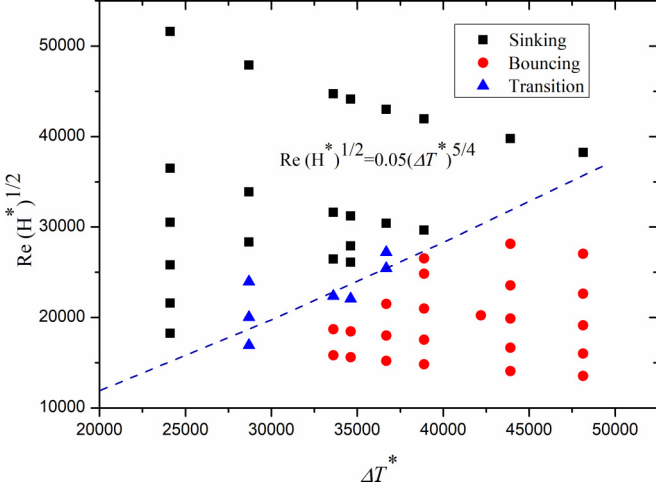


FIG. 3. Conditions when steel balls of different diameters (0.5/0.7/0.8/1 mm) and their release heights ( $L$ ) (5/10 mm) result in  $\text{Re}(H^*)^{0.5}$  values ranging from  $\sim 15000$  to  $55000$ , with dimensionless temperatures of  $\sim 3.0$ – $5.5$  ( $450$ – $600$  °C).

proportional to the vapor pressure:  $\rho_s R^3 a_s \sim \Delta P R^2$ , where  $a_s$  is the acceleration of a solid sphere and  $\rho_s$  is the density of a solid ball. After organizing and consolidating the information, the acceleration can be expressed as  $a_s \sim \frac{\Delta P}{\rho_s R}$ . The velocity of the solid sphere is  $U_s \sim a_s t$ , which can be determined based on the vapor pressure, steel-ball density, steel-ball radius, and time:  $U_s \sim \frac{\Delta P}{\rho_s R} t$ . According to Ref. [26], the bouncing time of the sphere is related to the dimensionless temperature ( $\Delta T^* = \frac{\rho_s C_p \Delta T}{\rho_g h_{fg}}$ ):

$$t \sim \frac{\rho_s C_p \forall^2}{K A^2} (\Delta T^*)^{1/4}. \quad (1)$$

Substituting the bouncing time above into the velocity expression of the solid sphere yields

$$U_s \sim \frac{\Delta P}{\rho_s R} \frac{\rho_s C_p \forall^2}{K A^2} (\Delta T^*)^{1/4}, \quad (2)$$

where  $C_p$  is the specific heat at constant pressure,  $K$  is the conductivity of the solid steel ball,  $\Delta T$  is the superheat,  $h_{fg}$  is the enthalpy of vaporization, and  $A$  and  $\forall$  are the area and volume of the solid steel ball, respectively. After incorporating two dimensionless parameters, i.e., the dimensionless temperature  $\Delta T^* = \frac{\rho_s C_p \Delta T}{\rho_g h_{fg}}$  and the vapor pressure of the Leidenfrost vapor layer  $\Delta p = \frac{24\mu R^2}{h^3} \left(-\frac{k\Delta T}{\rho_g L^2 h'}\right)$ , into the ultimate scaling law, we derived an expression correlating the inertial force and vapor pressure. This correlation is governed by the  $\text{Re}$ , dimensionless vapor thickness  $H^*$  ( $H^* = \frac{Ah'}{\forall}$ ), and dimensionless temperature  $\Delta T^*$ . The resulting equation is as follows:

$$\text{Re} \sim (H^*)^{-4} \Delta T^{*5/4}. \quad (3)$$

Using the vapor-pressure model to analyze of the motion of the sphere, we derived an expression correlating the  $\text{Re}$  and dimensionless parameters  $\Delta T^*$  and  $H^*$ . Subsequently, we applied this relationship to the data obtained from our experiments. The results are presented in Fig. 3, which shows that the results of scaling analysis matched

the experimental results. The relationship between the rebounding and nonrebounding (sinking) at the boundary is  $\text{Re}(H^*)^{1/2} = 0.05(\Delta T^*)^{5/4}$ . The experimental data indicating the boundaries between the two distinct types of impact behavior matched reasonably well with the scaling laws. Furthermore, sinking and rebounding occurred above and below this line, respectively. Our scaling laws indicate that spheres with lower superheat are likely to sink when they impact with higher inertia. However, spheres with higher superheat can bounce easily when the impact is mild. This is the focus of this letter, and we shall further discuss it in the next section. A distinct transition phenomenon was identified within the sinking and bouncing ranges. Additionally, for the impacting events without heating, we discovered that, even at room temperature, nonsinking may occur at low values of  $\text{Re}(H^*)^{1/2}$ . For nonheated regular droplets, surface tension can serve as a trampoline, i.e., the air layer remains stable at low impact velocities, whereas the droplet bounces below a certain Weber number.

The bouncing behavior of a heated sphere on a liquid surface primarily arises from the force generated by the vapor film of the sphere, as shown in Fig. 1(b). We assumed that the high-temperature surface of the sphere is like a superhydrophobic surface [25,34]. Moreover, regarding the inverse Leidenfrost effect, as discussed by Adda-Bedia *et al.* [22], we treat the Leidenfrost sphere as a perfectly nonwetting sphere ( $\theta = 180^\circ$ ). Therefore, we introduced a force model for a superhydrophobic sphere entering water. The magnitudes of these forces [35] are calculated based on the relative sizes of  $h$ ,  $\phi$ , and  $\beta$ , where  $\beta$  can be determined using geometric and angular relationships ( $\phi = \theta + \beta - \pi$ ). Therefore, when the location at which the sphere is released is known,  $\beta$  can be derived based on any position. Figure 4(a) shows the location of the center of the sphere  $h$  vs time;  $h$  is positive when the sphere traverses upward and zero at the undisturbed free surface. Further analysis of the force on the sphere yields the results depicted in Fig. 4(b). The hydrophobic sphere experiences various vertical forces in the following manner after descending into the water, including drag force  $F_{fd}(\frac{9}{16}\pi R^2 \rho \dot{h} \sin^4 \beta)$ , added-mass force  $F_m[-\frac{\pi}{6} R^3 \rho_f \ddot{h} A(\beta)]$ , weight force  $F_w(\frac{4}{3}\pi R^3 \rho_s g)$ , and surface tension  $F_s(2\pi R \gamma \sin \beta \sin \phi)$ . The added-mass force is the added inertia induced by the flows around the accelerating sphere [25]. As shown in Fig. 4(a), when the hot sphere descended into the free liquid surface (0 ms) until it reached its lowest position (7 ms), deceleration occurred owing to additional forces such as  $F_m$ ,  $F_{fd}$ , and  $F_s$ . We can infer that  $F_s$  is the dominant force, both during the upward and downward motions of the sphere. However, when the Leidenfrost phenomenon occurs, we cannot describe this phenomenon merely in terms of  $F_s$  owing to the presence of the vapor layer. In this letter, we refer to the pressure force caused by vapor, denoted as  $F_p$ , and utilize the vapor pressure formula presented in Ref. [17] as follows:

$$P = \frac{24\mu R^2}{h^3} \left[ -\frac{k\Delta T}{\rho_g h_{fg} h'} \right] \ln \left[ \frac{\cos(\frac{\beta}{2})}{\cos(\frac{\beta_m}{2})} \right]. \quad (4)$$



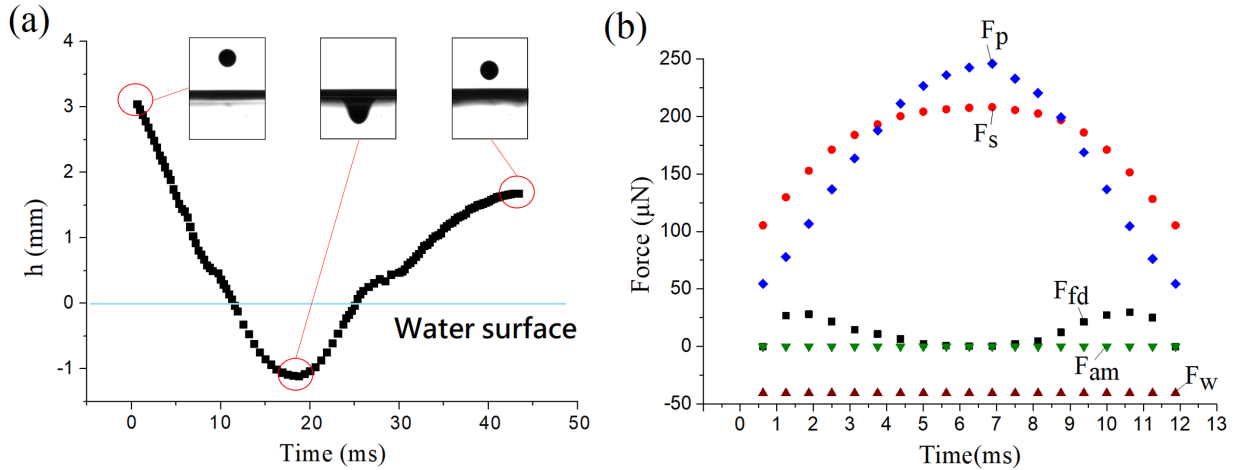


FIG. 4. (a) Location of sphere center  $h$  vs time. (b) Contribution of force components, including surface tension  $F_s$ , form drag  $F_{fd}$ , added-mass force  $F_{am}$ , weight force  $F_w$ , and pressure force  $F_p$ , for the case of a steel ball with a diameter of 1 mm released from a height of 0.5 cm at a surface temperature of  $600^\circ\text{C}$ .

The resultant force  $F_p$  exerted on the sphere by the vertical pressure is

$$F_p = 2\pi R^2 \int_0^{\beta_m} P \cos \beta \sin \beta d\beta, \quad (5)$$

where  $h'$  represents the air film thickness between the droplet and liquid surface, and  $\beta_m$  represents the maximum angular position. Assuming that the air film thickness was constant, we obtained a film thickness of  $\sim 50 \mu\text{m}$  via image analysis. We first observed the diameter of the sphere after it descended into the water at room temperature. Subsequently, we observed the diameter of the sphere when it descended into the water before being heated to the Leidenfrost temperature. The difference between the two yielded the thickness of the film. Figure 4(b) illustrates the force analysis of a steel ball with a diameter of 1 mm released from a height of 0.5 cm at a surface temperature of  $600^\circ\text{C}$ . We conclude that, at high temperature, the force exerted by the vapor pressure owing to the film is like the surface tension in the hydrophobic-sphere model.

To further validate the accuracy of the high-temperature sphere model, we employed Newton's second law [Eq. (6)] to evaluate the force relationship when a small steel ball bounced on the water surface. We determined the force relationship at the point where the speed of the ball reached zero, i.e., the position where the bounce speed began to increase. The value of all the resultant forces was  $2 \times 10^{-4} \text{ N}$ , which coincided with the values of the mass and acceleration of the ball at the current position. Additionally, we derived the relative position of the sphere underwater using Eq. (6). As shown in Fig. 5, the path of the steel ball with a diameter of 1 mm diameter was like the experimental path:

$$F_p + F_{am} + F_{fd} + F_w = \frac{4}{3}\pi R^3 \rho_s \ddot{h}. \quad (6)$$

When the temperature reached  $600^\circ\text{C}$  and the spheres were released from a height of 0.5 cm, all three spheres of different sizes bounced upward after reaching the free liquid surface. Figure 6(a) shows the height vs time graph for steel balls with diameters of 0.5, 0.7, and 1 mm released from a height

( $H$ ) of 0.5 cm at  $600^\circ\text{C}$ . The zero-height position was at the free liquid surface. By calculating the pressure difference  $P \propto \ln[\frac{1}{\cos(\frac{\beta_m}{2})}]$ , we observed as the steel-ball volume increased, the larger-diameter spheres submerged deeper. This indicates that a maximum pressure difference exists that results in forces. Figure 6(b) shows the forces experienced by spheres with diameters of 0.5, 0.7, and 1 mm when released from a height of 0.5 cm at  $600^\circ\text{C}$ . Therefore, the deformation of the free liquid surface is analogous to a spring undergoing deformation. As the deformation of the liquid surface increased, the pressure increased. Consequently, the energy experienced by the steel ball in the vertical direction increased with the radius, thus resulting in larger bounce heights. However, as the release height or the sphere diameter increased, with  $Re$  surpassing 37 927, the sphere motion may transition to excessive or regular sinking.

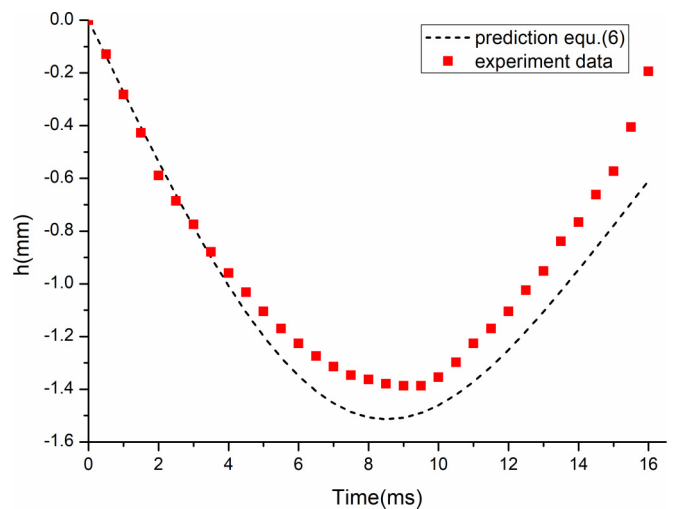


FIG. 5. Comparison between theoretical predictions (dashed lines) and experimental results (filled squares) of locations of sinking sphere (released from a height of 0.5 cm at a surface temperature of  $600^\circ\text{C}$ ).

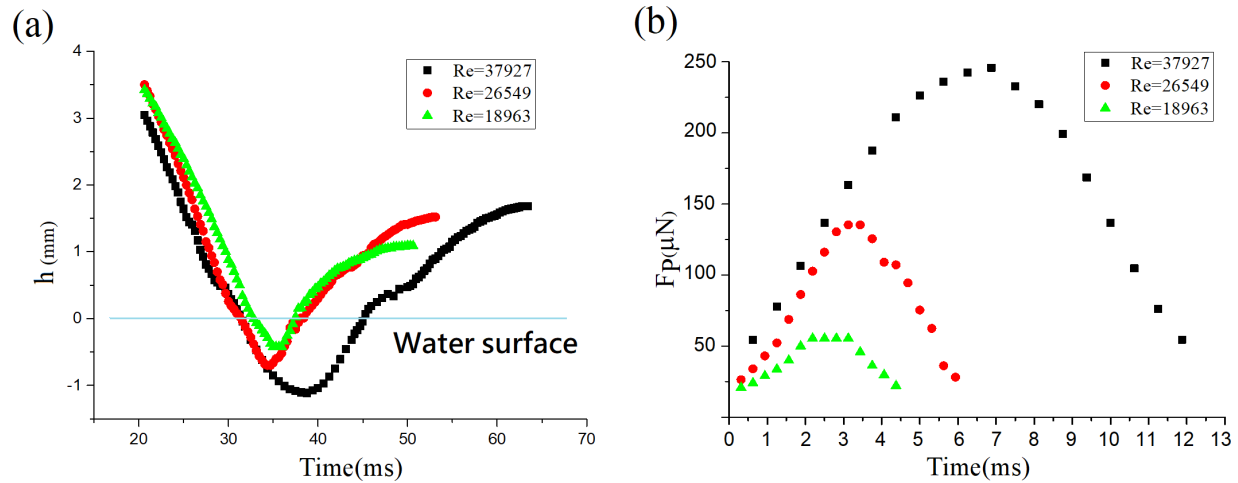


FIG. 6. (a) Paths of bouncing ball with  $Re = 37922$ ,  $26549$ , and  $18963$ . (b) Pressure experienced by sphere with  $Re = 37922$ ,  $26549$ , and  $18963$  during motion.

In this letter, we observed that elevated surface temperatures caused small solid spheres to bounce on the water surface. Based on force analysis, we inferred that the pressure force induced by the vapor on the surface of the sphere predominantly influenced the bouncing behavior. We identified three distinct motion behaviors for heated steel balls using three dimensionless parameters ( $Re$ ,  $H^*$ , and  $\Delta T^*$ ): sinking, transition, and bouncing. These motion behaviors, which are associated with the Leidenfrost effect of the spheres, may

contribute considerably to various future applications, including cooling, drag reduction, and liquid transport.

Data supporting the findings of this letter are available from the corresponding author upon request.

The authors acknowledge the financial support provided by the National Science and Technology Council of Taiwan (Grant No. NSTC 112-2221-E-239-021).

- [1] J. G. Leidenfrost, *De aquae communis nonnullis qualitatibus tractatus* (Ovenius, Duisburg, 1756).
- [2] G. G. Wells, R. Ledesma-Aguilar, G. McHale, and K. Sefiane, A sublimation heat engine, *Nat. Commun.* **6**, 6390 (2015).
- [3] M. Lan and X. Wang, A case study on the dynamic process of water drop impacting on heated wood surface, *Case Stud. Therm. Eng.* **2**, 23 (2014).
- [4] G. Kjaerheim, Heat transfer as limiting factor in water-cooled nuclear reactors, *Nucl. Eng. Des.* **21**, 279 (1972).
- [5] J. Kim, Spray cooling heat transfer: The state of the art, *Int. J. Heat Fluid Flow* **28**, 753 (2007).
- [6] G. Dupeux, M. Le Merrer, C. Clanet, and D. Quéré, Trapping Leidenfrost drops with crenulations, *Phys. Rev. Lett.* **107**, 114503 (2011).
- [7] H. Linke, B. J. Alemán, L. D. Melling, M. J. Taormina, M. J. Francis, C. C. Dow-Hygelund, V. Narayanan, R. P. Taylor, and A. Stout, Self-propelled Leidenfrost droplets, *Phys. Rev. Lett.* **96**, 154502 (2006).
- [8] A. Jetly, Ivan U. Vakarelski, Z. Yang, and Sigurdur T. Thoroddsen, Giant drag reduction on Leidenfrost spheres evaluated from extended free-fall trajectories, *Exp. Therm Fluid Sci.* **102**, 181 (2019).
- [9] Ali Hashmi, A. Hashmi, Y. Xu, B. Coder, P. A. Osborne, J. Spafford, G. E. Michael, G. Yu, and J. Xu, Leidenfrost levitation: Beyond droplets, *Sci. Rep.* **2**, 797 (2012).
- [10] M. Shi, X. Ji, S. Feng, Q. Yang, T. J. Lu, and F. Xu, Self-propelled hovercraft based on cold Leidenfrost phenomenon, *Sci. Rep.* **6**, 28574 (2016).
- [11] D. Attinger, C. Frankiewicz, A. R. Betz, T. M. Schutzius, R. Ganguly, A. Das, C.-J. Kim, and C. M. Megaridis, Surface engineering for phase change heat transfer: A review, *MRS Energy Sustain.* **1**, E4 (2014).
- [12] D. Quéré, Leidenfrost dynamics, *Annu. Rev. Fluid Mech.* **45**, 197 (2013).
- [13] A. Bouillant, B. Lafoux, C. Clanet, and D. Quéré, Thermophobic Leidenfrost, *Soft Matter* **17**, 8805 (2021).
- [14] B. Sobac, A. Rednikov, S. Dorbolo, and P. Colinet, Leidenfrost effect: Accurate drop shape modeling and refined scaling laws, *Phys. Rev. E* **90**, 053011 (2014).
- [15] G. Graeber, K. Regulagadda, P. Hodel, C. Küttel, D. Landolf, T. M. Schutzius, and D. Poulidakos, Leidenfrost droplet trampolining, *Nat. Commun.* **12**, 1727 (2021).
- [16] M. Faraday, On the relation of water to hot polished surfaces, *Q. J. Sci.* **1**, 221 (1828).
- [17] R. S. Hall, S. J. Board, A. J. Clare, R. B. Duffey, T. S. Playle, and D. H. Poole, Inverse Leidenfrost phenomenon, *Nature (London)* **224**, 266 (1969).
- [18] I. U. Vakarelski, J. O. Marston, D. Y. C. Chan, and S. T. Thoroddsen, Drag reduction by Leidenfrost vapor layers, *Phys. Rev. Lett.* **106**, 214501 (2011).
- [19] I. U. Vakarelski, N. A. Patankar, J. O. Marston, D. Y. C. Chan, and S. T. Thoroddsen, Stabilization of Leidenfrost vapour layer by textured superhydrophobic surfaces, *Nature (London)* **489**, 274 (2012).
- [20] I. U. Vakarelski, J. D. Berry, D. Y. C. Chan, and S. T. Thoroddsen, Leidenfrost vapor layers reduce drag without the

- crisis in high viscosity liquids, *Phys. Rev. Lett.* **117**, 114503 (2016).
- [21] I. U. Vakarelski, D. Y. C. Chan, and S. T. Thoroddsen, Leidenfrost vapour layer moderation of the drag crisis and trajectories of superhydrophobic and hydrophilic spheres falling in water, *Soft Matter* **10**, 5662 (2014).
- [22] M. Adda-Bedia, S. Kumar, F. Lechenault, S. Moulinet, M. Schillaci, and D. Vella, Inverse Leidenfrost effect: Levitating drops on liquid nitrogen, *Langmuir* **32**, 4179 (2016).
- [23] A. Gauthier, C. Diddens, R. Proville, D. Lohse, and D. van der Meer, Self-propulsion of inverse Leidenfrost drops on a cryogenic bath, *Proc. Natl. Acad. Sci. USA* **116**, 1174 (2019).
- [24] A. Bouillant, T. Mouterde, P. Bourriane, A. Lagarde, C. Clanet, and D. Quéré, Leidenfrost wheels, *Nat. Phys.* **14**, 1188 (2018).
- [25] D.-G. Lee and H.-Y. Kim, Impact of a superhydrophobic sphere onto water, *Langmuir* **24**, 142 (2008).
- [26] G. Birkhoff and R. Isaacs, Transient cavities in air-water entry, *Nav. Ordnance Rep.* **1490**, 68 (1951).
- [27] D. Gilbarg and R. A. Anderson, Influence of atmospheric pressure on the phenomena accompanying the entry of spheres into water, *J. Appl. Phys.* **19**, 127 (1948).
- [28] J. M. Aristoff and J. W. M. Bush, Water entry of small hydrophobic spheres, *J. Fluid Mech.* **619**, 45 (2009).
- [29] J. O. Marston, I. U. Vakarelski, and S. T. Thoroddsen, Cavity formation by the impact of Leidenfrost spheres, *J. Fluid Mech.* **699**, 465 (2012).
- [30] M. Castagna, N. Mazellier, and A. Kourta, Wake of superhydrophobic falling spheres: Influence of the air layer deformation, *J. Fluid Mech.* **850**, 646 (2018).
- [31] S. T. Thoroddsen, M.-J. Thoraval, K. Takehara, and T. G. Etoh, Micro-bubble morphologies following drop impacts onto a pool surface, *J. Fluid Mech.* **708**, 469 (2012).
- [32] G. Shakya, P. Dhar, and P. K. Das, Thermo-fluid-dynamics of inverse Leidenfrost levitation of small liquid/solid spheres over liquid pools, *Phys. Fluids* **35**, 042007 (2023).
- [33] See Supplemental Material at <http://link.aps.org/supplemental/10.1103/PhysRevE.110.L012802> for the video showing a ball of different sizes descending into water at different heating temperatures and release heights.
- [34] C. Huang, X. Wen, and M. Liu, Study on low-speed water entry of super-hydrophobic small spheres, *Chin. J. Theor. Appl. Mech.* **51**, 36 (2019).
- [35] D. Vella, D.-G. Lee, and H.-Y. Kim, Sinking of a horizontal cylinder, *Langmuir* **22**, 2972 (2006).